CrystEngComm

Accepted Manuscript

ROYAL SOCIETY OF CHEMISTRY

www.rsc.org/crystengcomm

Cite this: DOI: 10.1039/c0xx00000x

www.rsc.org/xxxxxx

ARTICLE TYPE

Tuning Sorption Properties *via* Activated Treatments in A Metastable Zn-1,3,5-Benzenetricarboxylate Framework with Dodecahedral and Cubic Cages

Huanqing Ma, Shujun Wang*, Hongyan Liu, Fanbin Meng, Wangang Zheng,Weiying Gao

Received (in XXX, XXX) Xth XXXXXXXXX 20XX, Accepted Xth XXXXXXXXX 20XX

DOI: 10.1039/b000000x

Present here is a metastable metal−organic framework built from the alternate connection of dodecahedral and cubic cages. For enhancing its sorption properties, three kinds of different activative treatments were performed to decrease the deleterious effect of solvent surface tension during activated processes.

Introduction

Porous metal−organic frameworks (MOFs), as a new generation of porous materials, have been widely used in the fields of gas storage/separation, catalysis, drug delivery, molecular recognition and sensor.[1] For the general applicability of as-synthesized MOFs, the preservation of permanent porosity after excitation should be the most important prerequisite and can be achieved by rational choice of activated treatments.[2] Although permanent porosity of the stable MOFs can often be attained by conventional vacuum-drying or heating after low-boiling solvents exchange, many metastable MOFs are apt to collapse into nonporous frameworks, clearly attributing to the strong solvent surface tension during the activated processes.[3] Therefore, how to eliminate the detrimental effect of surface tension during the activated processes may be extremely challenging. For this aim, Hupp and co-workers firstly employed supercritical carbon dioxide (SCD) process to significantly increase the surface areas of Zn-MOFs as the result of the low surface tension of SCD.[4] Subsequently, Lin's groups pioneered another special freeze-benzene drying treatment to tune the gas uptakes of two Cu-MOFs because such solid–gas transition can eliminate the detrimental effect of surface tension to enhance the permanent porosity of MOFs.[2] Recently, Zhang and co-workers comparatively studied how different activated methods, such as dichloromethane-exchange, freeze-cyclohexane drying and SCD activation, to affect gas sorption properties of a metastable MOF FIR-3.[5]

In this work, we report a new MOF, namely, $[Zn_{22}(btc)_{12}(H_2O)_{22}(NO_3)_8]\cdot x$guest (**1**), ($H_3$btc = 1,3,5-benzenetricarboxylate acid), which was built from the alternate connection of dodecahedral cages and cubic cages to form a high biporous framework with a void volume of 68.1% per unit cell. Owing to the metastable character, three different activative treatments, such as vacuum-drying, freeze-benzene drying,[2] and SCD activation, were carefully performed for **1** to investigate their impact on the tuning porosity and sorption propertoies of **1**. In addition, the gas selectivity of CO_2 over CH_4 for SCD activated sample was also investigated, giving a high selectivity of ~65.8.

Solvothermal reaction of $Zn(NO_3)_2\cdot 6H_2O$ with H_3btc in N,N'-diethylformamide (DEF) and ethanol (EtOH) afforded a high yield of colorless polyhedral crystals of **1**. The single-crystal diffraction analysis of **1** crystallized in centrosymmetric cubic

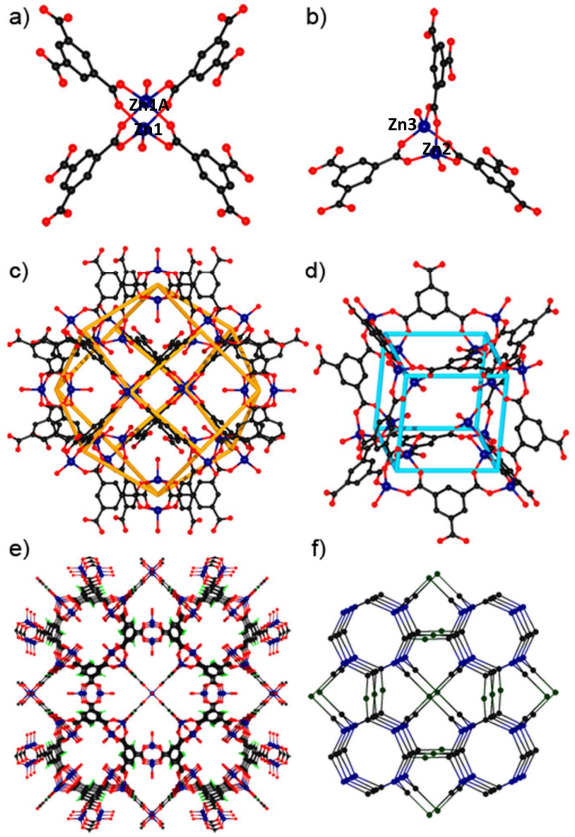

Figure 1. a) the coordination modes of four-connected $Zn_2(COO)_4$ SBUs and b) three-connected $Zn_2(COO)_3$ SBUs (Zn: dark blue, O: red, C: black); c) a dodecahedral cage in **1**; d) a cubic cage in **1**; e) View of the bi-porous framework of **1** viewed close to [100] direction; f) schematic representation of the ***tfe*** topological net of **1** (viewed close to the [100] direction; green balls representing four-connected $[Zn_2(COO)_4(H_2O)_2]$ nodes, blue ones representing the 3-connected $[Zn_2(COO)_3(H_2O)_2]$ nodes and black ones representing 3-connected btc ligands).

space group *Pm-3m* reveals a three dimensional (3D) (3,4)-connected coordination framework, in which there are two types of second building units (SBUs). One is the typical four-connected paddlewheel $[Zn_2(COO)_4(H_2O)_2]$ unit, in which each Zn ions is bonded by four carboxylate groups from four btc ligands and one water molecule to form a square-pyramidal geometry (Figure 1a), which is widely known in the HKUST-1, MOF-14 and many other MOFs.[6-8] In the paddlewheel unit, the Zn1-O bond lengths vary from 1.991(4) to 2.020(4) Å and the Zn···Zn distance is 2.9855(5) Å, which is slightly longer than conventional paddlewheel species (ca. 2.65 Å). Another $[Zn_2(COO)_3(H_2O)_2]$ unit is an cationic three-connected unit, in which each Zn center is coordinated with three carboxylate O atoms from three different btc ligands and one water molecule to form a tetrahedral geometry (Figure 1b). The Zn2-O and Zn3-O bond lengths vary from 1.8954(4) to 1.9365(4) Å and the distance of Zn2···Zn3 bridged by three carboxylate groups is 3.5170(5) Å. This $Zn_2(COO)_3(H_2O)_2$ unit is interesting and rarely seen in other MOFs.[9] One prominent structural feature in **1** is the presence of two kinds of cages. The large cage consists of six $Zn_2(COO)_4$ SBUs as four-connected vertexes and eight $Zn_2(COO)_3$ SBUs as three-connected vertexes, forming a rhombic dodecahedron if twenty-four btc ligands are considered as the edges (Figure 1c and S1, ESI). The rhombic window of the dodecahedron containing two $Zn_2(COO)_4$ SBUs and two $Zn_2(COO)_3$ SBUs as vertexes is not completely coplanar. The interior cavity of the dodecahedron is about 15 Å (Figure 1c and S1, ESI). The small cage is built from eight $Zn_2(COO)_3$ SBUs to form a cube with the interior cavity of about 10 Å, where eight $Zn_2(COO)_3$ SBUs are considered as three-connected vertexes and twelve btc ligands are used for the edges (Figure 1d and S2, ESI). The square windows in this cubic cage are completely coplanar. To the best of our knowledge, MOFs that coexist these two different polyhedrons are rarely reported. Interestingly, such adjacent dodecahedron and cube are corner-sharing to each other (Figure S3, ESI). Thus, each dodecahedral or cubic cage as super SBU is further linked to other eight adjacent cubic or dodecahedral cages through their shared $Zn_2(COO)_3$ corners, generating a biporous and positive 3D framework (Figure 1e). The void volume of **1** without guest molecules and NO_3^- anions is 68.1% per unit cell calculated by PLATON.[10] The overall structure of **1** can be described as a (3,4)-connected ***tfe***-like network with the Schläfli symbol of $\{8^3\}_{20}\{8^4;12^2\}_3$ by topologically simplifying each $[Zn_2(COO)_4(H_2O)_2]$ unit, $[Zn_2(COO)_3(H_2O)_2]$ unit and btc ligand as the 4-, 3- and 3-connected node, respectively (Figure 1f).

To prove that the crystal structure of **1** can be take as truly representative of the bulk sample, X-ray powder diffraction (XRPD) experiments were carried out on the as-synthesized **1**. The XRPD experimental patterns of **1** are in good agreement with the simulated one (Figure S4a and S4b, ESI). At the same time, to investigate the thermal stability of **1**, the thermogravimetric analysis (TGA) experiment was carried out in the temperature range from 25 to 600 °C under a flow of nitrogen with a heating rate of 10 °C/min. The TGA curve of **1** shows a continual weight loss without an obvious plateau (Figure S5, ESI). Due to the high evacuated temperature of the guest, the as-synthesized **1** was activated by immersing in dichloromethane (CH_2Cl_2) for 7 days and then outgassed overnight under high vacuum and room temperature to generate dehydrated form **1a**, whose PXRD pattern is obviously different from that of **1** (Figure S4c, ESI), indicating the relaxation or collapse of the high-porous framework effected by strong solvent surface tension during the activated process. To decrease the deleterious effect of solvent surface tension during the guest releasing process, the freeze-benzene drying and SCD experiments according to previous reported methods were used to activate the original **1**, giving two new activated phases **1b** and **1c**, respectively (Experimental Section in ESI).

Different activation treatments of **1** provide a great opportunity to make a comparative study on tuning porosity for gas sorption. The N_2 adsorption isotherms for activated **1a**, **1b** and **1c** were collected to determine that how the activation treatments impact the pore volume and surface area (Figure 2a). The N_2 sorption isotherm for **1a** shows a typical external adsorption behavior at 77 K. However, the N_2 sorption isotherms for **1b** and **1c** reveal reversible type-I sorption behavior of microporous materials characterized by a plateau reached at low relative pressure (Figure 2b-c), giving maximum uptakes of 27.7 cm^3/g for **1b** and

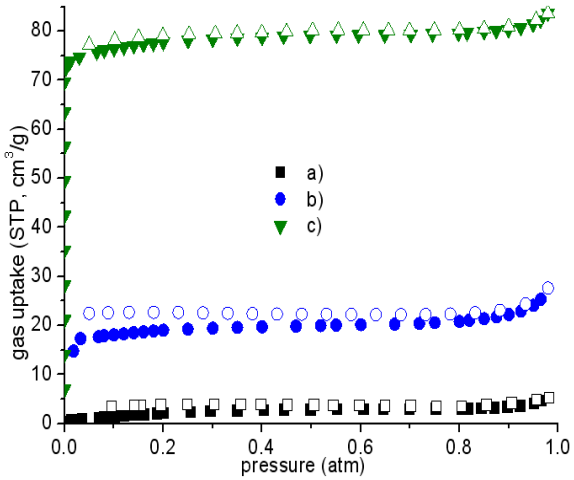

Figure 2. N_2 sorption isotherms for **1a** (a), **1b** (b) and **1c** (c) at 77 K.

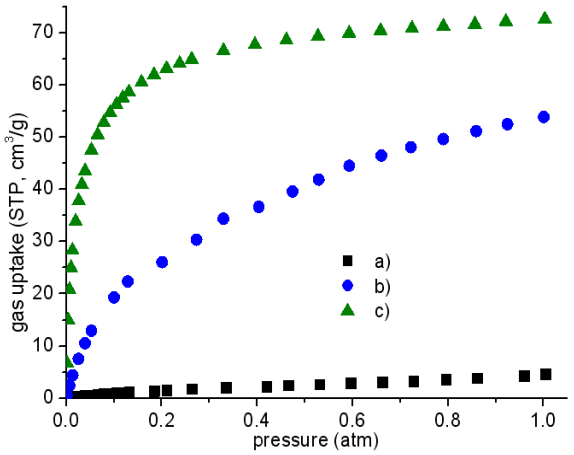

Figure 3. H_2 sorption isotherms for **1a** (a), **1b** (b), and **1c** (c) at 77 K.

77.2 cm^3/g for **1c**, which are much higher than that (5.4 cm^3/g) of **1a**. The Langmuir surface areas are calculated to be 86.9 m^2/g for **1b** and 343.9 m^2/g for **1c**, which are about 5- and 21-fold enhancement over the regular vacuum-dried sample **1a**, respectively. The given single point adsorption total pore volumes at P = 0.98 atm for **1b** and **1c** are 0.043 and 0.129 cm^3/g, respectively, confirming there are accessible micropores in **1b** and **1c**. However, the above values of pore volumes and Langmuir surface areas are much smaller than the theoretical pore volume (0.81 cm^3/g) and surface area (3334 m^2/g) calculated by Materials Studio 6.0, respectively. These freeze-benzene drying and SCD activated MOFs also show a significantly enhanced H_2 uptake capacity (Figure 3). For example, H_2 uptake for freeze-benzene dried **1b** increased to 53.9 cm^3/g, nearly be twelve times as large as the value of the vacuum-dried **1a** (4.7 cm^3/g), and SCD activated **1c** shows the highest H_2 uptake of 72.6 cm^3/g. Compared to some stable MOFs,[5] the above gas uptakes, surface areas and pore volumes are all inferior, indicating that the host framework of **1** inevitably undergoes significant pore relaxation or collapse regardless of the mildest SCD activated treatment. However, the decrease of the detrimental effect of surface tension during activated processes can help to protect the integrity of the high porous frameworks and enhance sorption properties.

The CO_2 sorption isotherms for **1c** were also measured at 273 and 298 K under 1 atm. As shown in Figure 4, the CO_2 capacity of **1c** is 58 cm^3/g at 273 K and 1 bar. The enthalpy of CO_2 adsorption for **1c** is estimated from the sorption isotherms at 273 and 298 K by using the virial equation (Figure S7 and S8, ESI). The isosteric heat of CO_2 adsorption for **1c** achieves a value of 28 kJ/mol, which is comparable to those of MOFs with organic ammonium ions in the pores for strong CO_2 binding.[11] However, the CH_4 uptake of **1c** is just 8 cm^3/g under 298 K and 1 atm, indicating that **1c** as a promising material can effectively separate CO_2 from CH_4. To evaluate the CO_2/CH_4 selectivity of **1c** under mixture gas conditions with single-component isotherms, the ideal adsorbed solution theory (IAST) can be used to predict multicomponent adsorption behaviors. The experimental data are fits of the dual-site Langmuir–Freundlich mode (Figure S9, ESI) and the predicted selectivity for equimolar CO_2/CH_4 gas mixture pairs in **1c** are plotted in Figure 4d. It is remarkable that **1c** shows very high CO_2/CH_4 selectivity of ~65.8, which can close to a recently reported 2-fold interpenetrated microporous MOF,[12] and is much higher than some reported MOF materials under similar conditions, such as a Co(II) carborane-based MOF (~47),[13] HKUST-1 (~8),[14] MIL-53(Cr) (~9).[15] It is noted that the high selective separation of CO_2/CH_4 suggests that **1c** may be used for natural gas purification.

In summary, a metastable framework **1** built from the alternate connection of dodecahedral cages and cubic cages is synthetized. a comparative study of activation methods on tuning gas sorption properties of **1** is successfully investigated. What is more, SCD-activated **1c** shows a remarkable CO_2/CH_4 selectivity of ~65.8 under 298 K and 1 atm. The results demonstrate activative treatmenst play an important role on tuning stability and porosity of metastable MOFs.

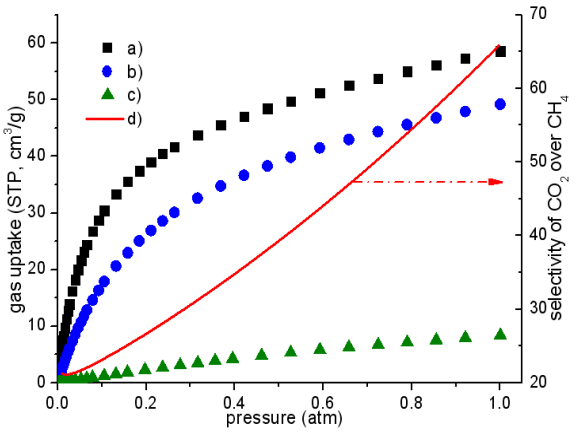

Figure 4. gas sorption isotherms for **1c**: a) CO_2 at 273 K; b) CO_2 at 298 K; c) CH_4 at 298 K; d) the predicted selectivities for equimolar CO_2/CH_4 gas mixture pairs for **1c** at 298 K.

Acknowledgements

The authors gratefully thank the financial support of State Key Laboratory of Heavy Oil Processing in China University of Petroleum-Beijing.

Notes and References

State Key Laboratory of Heavy Oil Processing, China University of Petroleum (Beijing), Beijing 102249, China.
E-mail: mahuanqinggg@163.com; bjwsjbj@sina.com

Electronic supplementary information (ESI) for this article is available: detailed experimental procedures, additional figures, TGA curve, PXRD patterns, CCDC reference number: 1030956, crystallographic data in cif and other electronic format seen DOI: 10.1039/b000000x/

1 (a) C. D. Wu and W. Lin, *Angew. Chem., Int. Ed.*, 2005, **44**, 1958-1961; (b) X. Feng, X. Ding and D. Jiang, *Chem. Soc. Rev.*, 2012, **41**, 6010-6022; (c) Y. Q. Chen, G. R. Li, Z. Chang, Y. K. Qu, Y. H. Zhang and X. H. Bu, *Chem. Sci.,* 2013, **4**, 3678-3682; (d) Q. Chen, Z. Chang, W. C. Song, H. Song, H. B. Song, T. L. Hu and X. H. Bu, *Angew. Chem., Int. Ed.*, 2013, **52**, 11550-11553; (e) B. L. Chen, S. C. Xiang and G. D. Qian, *Acc. Chem. Res.,* 2010, **43**, 1115-1124.

2 L. Ma, A. Jin, Z. Xie and W. Lin, *Angew. Chem., Int. Ed..*, 2009, **48**, 9905-9908.

3 J. Liu, B. Lukose, O. Shekhah, H. K. Arslan, P. Weidler, H. Gliemann, S. Brase, S. Grosjean, A. Godt, X. Feng, K. Mullen, I. B. Magdau, T. Heine and C. Woll, *Sci. Rep.*, 2012, **2**, 921, DOI: 10.1038/srep00921.

4 A. P. Nelson, O. K. Farha, K. L. Mulfort and J. T. Hupp, *J. Am. Chem. Soc.*, 2009, **131**, 458-460.

5 Y.-P. He, Y.-X. Tan and J. Zhang, *Inorg. Chem.*, 2012, **51**, 11232-11234.

6 S. S.-Y. Chui, S. M.-F. Lo, J. P. H. Charmant, A. G. Orpen and I. D. Williams, *Science*, 1999, **283**, 1148-1150.

7 B. Chen, M. Eddaoudi, S. T. Hyde, M. O'Keeffe and O. M. Yaghi, *Science*, 2001, **291**, 1021-1023.

8 (a) X. Lin, I. Telepeni, A. J. Blake, A. Dailly, C. M. Brown, J. M. Simmons, M. Zoppi, G. S. Walker, K. M. Thomas, T. J. Mays, P. Hubberstey, N. R. Champness and M. Schroder, *J. Am. Chem. Soc.*, 2009, **131**, 2159-2171; (b) X. Lin, A. J. Blake, C. Wilson, X. Z. Sun, N. R. Champness, M. W. George, P. Hubberstey, R. Mokaya and M. Schroder, *J. Am. Chem. Soc.*, 2006, **128**, 10745-10753; (c) X. Chen, S. He, F. Chen and Y. Feng, *CrystEngComm*, 2014, **16**, 8706-8709.

9 (a) Y. Liu, W. Xuan, H. Zhang and Y. Cui, *Inorg. Chem.*, 2009, **48**, 10018–10023; (b) Y.-P. He, Y.-X. Tan, F. Wang, J. Zhang, *Inorg. Chem.*, 2012, **51**, 1995–1997; (c) X. L. Zhao, H. Y. He, F. N. Dai, D. F. Sun and Y. X. Ke, *Inorg. Chem.,* 2010, 49, 8650-8652.

10 A. L. Spek, *J. Appl. Crystallogr.,* 2003, **36**, 7-13.

11 Y. X. Tan, Y. P. He and J. Zhang, *Chem. Commun.*, 2011, **47**, 10647–10649.
12 B. Chen, S. Ma, E. J. Hurtado, E. B. Lobkovsky and H. C. Zhou, *Inorg. Chem.*, 2007, **46**, 8490-8492.
13 Y. S. Bae, A. M. Spokoyny, O. K. Farha, R. Q. Snurr, J. T. Hupp and C. A. Mirkin, *Chem. Commun.*, 2010, **46**, 3478-3480.
14 C. Prestipino, L. Regli, J. G. Vitillo, F. Bonino, A. Damin, C. Lamberti, A. Zecchina, P. L. Solari, K. O. Kongshaug and S. Bordiga, *Chem. Mater.*, 2006, **18**, 1337-1346.
15 S. Bourrelly, P. L. Llewellyn, C. Serre, F. Millange, T. Loiseau and G. Ferey, *J. Am. Chem. Soc.*, 2005, **127**, 13519-13521.

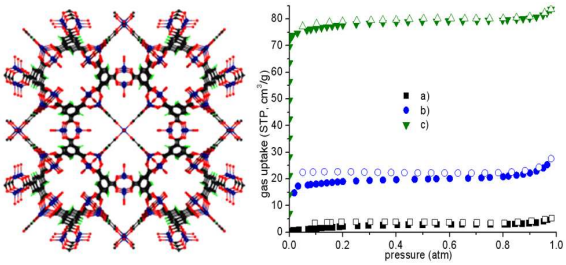

Presented here is a metastable MOF built from the alternate connection of dodecahedral and cubic cages. Three different activative treatments, vacuum-drying, freeze-benzene drying and SCD activation, were performed to optimize the porosity and gas uptakes of the metastable MOF.